



Implementing Multi-scale AGricultural INDicators Exploiting Sentinels

## **VALIDATION REPORT FOR THE GLOBAL LAND DATA ASSIMILATION SYSTEM OPERATED BY ECMWF**

IMAGINES\_RP7.4\_Validation-LDAS

### **ISSUE I1.00**

EC Proposal Reference N° FP7-311766

Due date of deliverable: 30.06.2015

Actual submission date: 21.09.2015

Start date of project: 01.11.2012

Duration : 40 months



Name of lead partner for this deliverable:

Book Captain: Gianpaolo Balsamo

Contributing Authors: Souhail Boussetta

<b>Project co-funded by the European Commission within the Seventh Framework Program (2013-2017)</b>		
<b>Dissemination Level</b>		
PU	Public	<b>X</b>
PP	Restricted to other programme participants (including the Commission Services)	
RE	Restricted to a group specified by the consortium (including the Commission Services)	
CO	Confidential, only for members of the consortium (including the Commission Services)	

## DOCUMENT RELEASE SHEET

Book Captain:	G. Balsamo	Date: 21.09.2015	Sign. 
Approval:	R. Lacaze	Date: 24.09.2015	Sign. 
Endorsement:	I. Marin-Moreno	Date:	Sign.
Distribution:	Public		

## CHANGE RECORD

Issue/Revision	Date	Page(s)	Description of Change	Release
	21.09.2015	All	First issue	I1.00

## TABLE OF CONTENTS

---

<b>1.</b>	<b><i>Background of the Document</i></b> .....	<b>9</b>
1.1.	Executive Summary .....	9
1.2.	Scope and Objectives.....	10
1.3.	Content of the Document .....	10
1.4.	Related Documents .....	10
1.4.1.	Inputs.....	10
1.4.2.	Output .....	10
<b>2.</b>	<b><i>Validation framework</i></b> .....	<b>11</b>
2.1.	Introduction .....	11
2.2.	Inter-annual variability and extreme events monitoring .....	12
2.3.	Drought and agriculture indicators .....	14
2.3.1.	Net ecosystem exchange and above-ground biomass indicators .....	14
2.3.2.	Comparison with WOFOST products.....	16
2.4.	Energy and water .....	18
2.4.1.	Energy and carbon Fluxes.....	19
2.4.2.	Soil moisture.....	21
2.5.	Forecast impact of Global Land products .....	22
<b>3.</b>	<b><i>Conclusions and Perspectives</i></b> .....	<b>26</b>
<b>4.</b>	<b><i>References</i></b> .....	<b>27</b>
	<b><i>Acknowledgement</i></b> .....	<b>29</b>

## LIST OF FIGURES

---

<i>Figure 1: Anomaly Index [%] with respect to mean (1999-2013) climate of LAI (left) and broadband diffuse albedo (right) for a) August 2003, b) July 2010 and c) November 2010. Regions of interest are zoomed in. ....</i>	13
<i>Figure 2: Above ground biomass-based Anomaly Index (<math>AI_{AGB}</math>) for November 2010 in [%] of the 1999-2013 mean. ....</i>	14
<i>Figure 3: Time series of the Net Ecosystem Exchange anomaly [<math>\mu\text{moles m}^{-2} \text{s}^{-1}</math>] for the Horn of Africa (left), and for central Australia (right). Anomalies are shown as differences of absolute flux between simulation using climatological LAI and albedo and simulation using global LDAS. ....</i>	15
<i>Figure 4: Comparison between WOFOST (black), CTESSEL with climatological LAI and albedo (green) and global LDAS (red) for the above-ground biomass (upper panel) and its anomaly with regard to the 1999-2013 mean (lower panel) at a FLUXNET Hungarian site. ....</i>	17
<i>Figure 5: Same as Figure 4 for a FLUXNET Portuguese site. ....</i>	18
<i>Figure 6: Latent Heat flux [<math>\text{W m}^{-2}</math>] for November 2010, a) using climatological LAI and albedo (SCLIM). Anomalies are shown as differences of absolute fluxes with respect to SCLIM for simulations using b) LAI and albedo NRT assimilation (SNRT), c) LAI NRT assimilation and albedo climatology (SLAINRT) and d) albedo NRT assimilation and LAI climatology (SLABNRT). ....</i>	19
<i>Figure 7: Similar to Figure 6 for the Sensible Heat flux [<math>\text{W m}^{-2}</math>]. ....</i>	20
<i>Figure 8: Scores of forecast experiment using LDAS LAI (FLAINRT) against experiment using LAI climatology (FCLIM) for November 2010: a) 2-m temperature sensitivity [K], b) 2-m relative humidity sensitivity [%], c) 2-m temperature impact, and d) 2-m relative humidity impact. (A positive/negative value of the impact means an increase/reduction of the 2-m temperature/relative humidity error in comparison to the operational analysis). ....</i>	24
<i>Figure 9: Scores of forecast experiment using LDAS LAI and albedo (FNRT) against experiment using climatology (FCLIM) for November 2010: a) 2-m temperature sensitivity [K], b) 2-m relative humidity sensitivity [%], c) 2-m temperature impact, and d) 2-m relative humidity impact. (A positive (negative) value of the impact means an increase (reduction) of the 2-m temperature/relative humidity error in comparison to the operational analysis). ....</i>	25

## LIST OF TABLES

---

*Table 1: Flux evaluation averaged against 52 FLUXNET sites for 2003: metrics based on 10-day averaged simulated fluxes. The Confidence Interval (CI) of RMSE is based on the Chi-squared distribution and the 95% CI of the mean correlation is based on the Fisher Z ..... 21*

*Table 2: Averaged metrics for surface and root-zone soil moisture benchmarking against the ISMN sites for 2010 based on daily soil moisture values. The confidence Interval (CI) of RMSE is based on the Chi-squared distribution and the 95% CI of the mean correlation is based on the Fisher Z. .... 22*

## ACRONYMS

---

ECMWF (European Centre for Medium-Range Weather Forecasts)  
CTESSEL (Carbon-Hydrology Tiled ECMWF Scheme for Surface Exchanges over Land)  
CGMS (Crop Growth Monitoring System)  
GEOGLAM (the Global Agricultural Geo-Monitoring Initiative)  
GEOV1 (Version 1 of LAI, FAPAR, FCover products)  
IFS (Integrated forecasting system)  
ISMN (International Soil Moisture Network)  
JRC (Joint Research Center)  
LAI (Leaf Area Index)  
LDAS (Land Data Assimilation System)  
LSM (Land Surface Model)  
MARS (Monitoring Agricultural ResourceS)  
NWP (Numerical Weather Prediction)  
RMSE (Root Mean Square Error)  
SSM (Surface soil moisture)  
USCRN (United State Climate Reference Network)  
VEGETATION (The medium resolution sensor onboard SPOT4 and SPOT5)  
WOFOST ( WORld FOod STudies)



## 1. BACKGROUND OF THE DOCUMENT

### 1.1. EXECUTIVE SUMMARY

The Copernicus program is the EU response to the increasing demand for reliable environmental data. The objective of the Copernicus Land Service is to continuously monitor and forecast the status of land territories and to supply reliable geo-information to decision makers, businesses and citizens to define environmental policies and take right actions. ImagineS intends to continue the innovation and development activities to support the operations of the Copernicus Global Land service, preparing the use of the new Earth Observation data, including Sentinels missions data, in an operational context. Moreover, ImagineS aims to favor the emergence of downstream activities dedicated to the monitoring of crop and fodder production, which are key for the implementation of the EU Common Agricultural Policy, of the food security policy, and could contribute to the Global Agricultural Geo-Monitoring Initiative (GEOGLAM) coordinated by the intergovernmental Group on Earth Observations (GEO).

The main objectives of IMAGINES are to (i) improve the retrieval of basic biophysical variables, mainly LAI, FAPAR and the surface albedo, identified as Terrestrial Essential Climate Variables, by merging the information coming from different sensors (PROBA-V and Landsat-8) in view to prepare the use of Sentinel missions data; (ii) develop qualified software able to process multi-sensor data at the global scale on a fully automatic basis; (iii) explore new paths to complement and contribute to the existing or future agricultural services by providing new data streams relying upon an original method to assess the above-ground biomass, based on the assimilation of satellite products in a Land Data Assimilation System (LDAS) to monitor the crop/fodder biomass production together with the carbon and water fluxes; (iv) demonstrate the added value of this contribution for a community of users acting at global, European, national, and regional scales.

The added value of the assimilation of satellite products on vegetation biomass and carbon fluxes is evaluated at the global scale based on assessment against known extreme events. In addition, a benchmarking of the above-ground biomass issued from the Global LDAS at local sites was performed against the WOrld FOod Studies (WOFOST) products. It is shown that the LDAS is able to better capture/monitor extreme events and that the assimilation of LAI improves of the correlation between the simulated above-ground biomass and the WOFOST products.

Furthermore, it is shown that the assimilation of LAI have a positive impact on surface fluxes and near surface atmospheric variables. This impact tends to become negligible when assimilating the surface albedo.

## 1.2. SCOPE AND OBJECTIVES

Surface observations and known extreme events are used to assess and validate the Global LDAS outputs in term of drought/agriculture and Numerical Weather Prediction (NWP). In addition, simulations from the WOFOST crop model are used as a benchmark for the above-ground biomass outputs.

## 1.3. CONTENT OF THE DOCUMENT

The Chapter 2 presents the validation framework of the Global LDAS for agriculture, drought and NWP. Conclusions and prospects are presented in Chapter 3.

## 1.4. RELATED DOCUMENTS

### 1.4.1. Inputs

Overview of former deliverables acting as inputs to this document.

Document ID	Descriptor
ImagineS_RP1.1	Users Requirements Document
ImagineS_RP1.2	Service Specifications Document
ImagineS_RP3.1	LDAS ATBD

### 1.4.2. Output

Overview of other deliverables for which this document is an input:

Document ID	Descriptor
ImagineS_RP6.3	Product User Manual of LDAS output products

## 2. VALIDATION FRAMEWORK

### 2.1. INTRODUCTION

As a fundamental component of a land surface model (LSM), the vegetation layer plays a crucial role in the land–atmosphere exchanges. The vegetation contributes to the evaporation through the plant transpiration and direct evaporation of the plant-intercepted precipitation. It affects also the available surface energy through the radiative transfer within the canopy by modifying the surface albedo (Deardorff, 1978). On the other hand, the exchanges of water vapour and CO<sub>2</sub> with the atmosphere drive the state of soil moisture and vegetation and thus the agriculture outputs.

In most LSMs, the Leaf Area Index (LAI) is used as an indicator of the vegetation state (e.g. greening, mature, senescent, and dormant). Subsequently, with soil moisture, LAI is considered as a key factor controlling the water, energy and carbon cycles.

In addition, the surface albedo was shown to be one of the important parameters that controls not only land surface energy balance and affects the atmospheric boundary layer through the surface radiative balance (Pielke & Avissar, 1990), but also the carbon cycle through its control of the available energy to plant photosynthesis.

The usage of satellite derived LAI, soil moisture and surface albedo within LSMs was shown to have a positive impact on LSM and NWP system (Balsamo et al. 2009, Balsamo et al. 2011, Boussetta et al. 2013, de Rosnay et al., 2013, Barbu et al. 2014), hydrological models (Draper et al., 2011, Sawada et al. 2014) and agricultural models (Bolten and Crow, 2012, Calvet et al. 2012).

The scientific validation aims to assess the reliability (spatial and temporal) of the products, determine accuracy and precision of the products, identify problematic areas and possible cause of errors, analyse the compliance regarding users requirements, and provide recommendations on the usability of the products. It has been shown that:

- i. The Copernicus Global Land Service LAI and albedo products when ingested within the Global LDAS are able to detect and monitor drought and extreme events at global and regional scale.
- ii. The Global LDAS is able to produce new drought indicators useful for agriculture yield monitoring based on Net Ecosystem Exchange and above-ground biomass.

- iii. The assimilation of the LAI within the Global LDAS tends to improve the prediction of the near surface atmosphere when coupled to NWP system.

## 2.2. INTER-ANNUAL VARIABILITY AND EXTREME EVENTS MONITORING

The temporal and spatial consistency is assessed through the assimilation of NRT LAI and surface albedo products, provided by the Copernicus Global Land service, within the ECMWF system. The assimilation results confirm that the NRT LAI and albedo outputs have smooth and realistic fields that are capable of mimicking their inter-annual variability and correctly detect and monitor extreme events.

Figure 1 displays the anomaly Index  $AI_V = \frac{V_i - \bar{V}_{i,1999-2013}}{\bar{V}_{i,1999-2013}} * 100$  of the assimilated LAI

(left panel) and albedo (right panel) with regard to their 1999–2013 climatologies for three known extreme event cases: the 2003 European drought (upper panel), the 2010 Russian summer heat wave (middle panel) and the 2010 Horn of Africa drought which occurred at the same period as a drought recovery in Australia (lower panel). Figure 1 shows that for these cases, the LAI anomaly is generally more pronounced than the albedo anomaly. The LAI anomaly can reach 80% of the climatological values, whereas the albedo anomaly does not exceed 20%. In addition, the albedo anomaly is more pronounced in extreme wet cases such as in central Australia during the wet period of November 2010 where the anomaly reached -10%, while LAI anomaly is perceptible in both dry and wet cases (e.g. the anomaly during the Horn of Africa drought reached -40% and the anomaly over the central Australia attained +40% of the climatological values). Owing to the soil background exposure compensation which also depends on the soil type and moisture, the link between LAI anomaly and albedo anomaly is not always clear. However, Figure 1 shows that a positive LAI anomaly is generally associated with a negative albedo anomaly in low vegetation areas. 20% to 40% LAI positive anomaly corresponds to a 1% to 10% negative albedo anomaly depending on the low vegetation type and cover. These results showed that the assimilation system is able to correct deficiencies in the satellite observation product, especially in high latitudes and snow covered areas as well as in the cloud-contaminated areas. The final products have smoother spatial and temporal evolution, which make them more appropriate for hydrological, agricultural and numerical weather prediction.

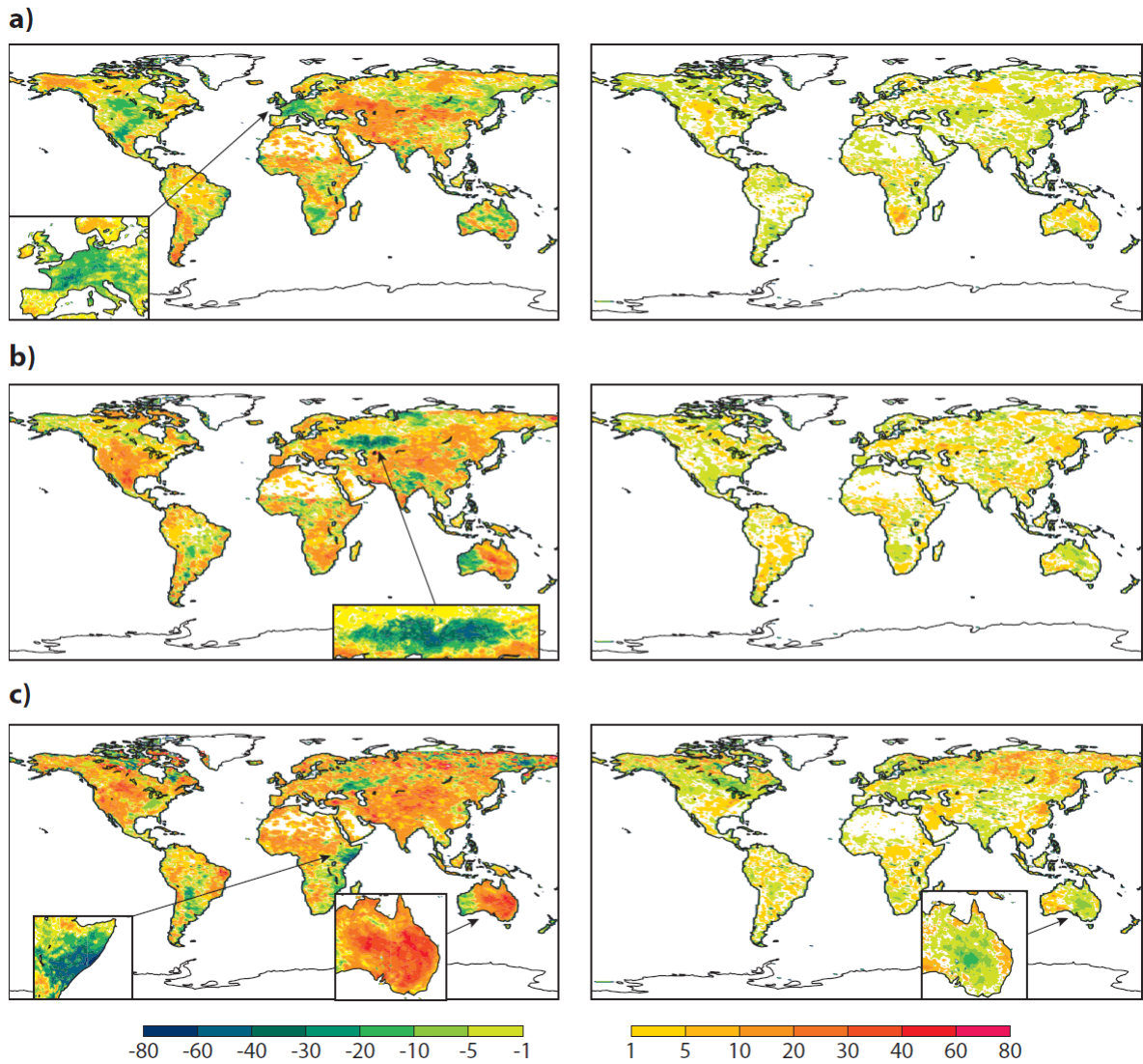


**Figure 1: Anomaly Index [%] with respect to mean (1999-2013) climate of LAI (left) and broadband diffuse albedo (right) for a) August 2003, b) July 2010 and c) November 2010. Regions of interest are zoomed in.**

## 2.3. DROUGHT AND AGRICULTURE INDICATORS

Soil moisture products, biomass and carbon fluxes are directly linked to agriculture growth and drought status. Therefore, we mainly focus on these parameters to assess the efficiency of the Global LDAS in tracking growth variability and drought events. Drought indicators based on above-ground biomass, NEE and soil moisture were assessed against known extremes. In addition, a benchmarking of the above-ground biomass issued from the Global LDAS at local sites was performed against the World Food Studies (WOFOST) products which are currently developed by the Crop Growth Monitoring System (CGMS) within the Monitoring Agricultural Resources unit (MARS) of the JRC.

### 2.3.1. Net ecosystem exchange and above-ground biomass indicators

The anomaly Index was shown to be a good indicator of the vegetation status and extreme events.

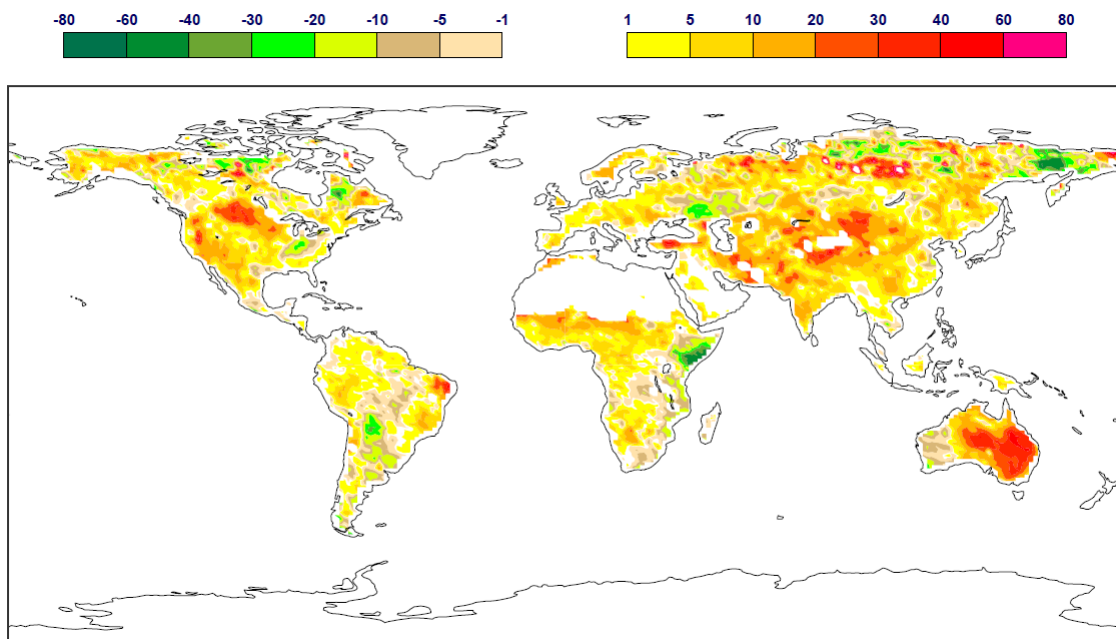


**Figure 2: Above ground biomass-based Anomaly Index ( $AI_{AGB}$ ) for November 2010 in [%] of the 1999-2013 mean.**



Figure 2 shows November 2010 above-ground biomass based anomaly Index ( $AI_{AGB}$ ) with regard to the 1999-2013 mean. November 2010 is characterized by a drought in the Horn of Africa and a wet event corresponding to drought recovery in central and eastern Australia as identified in Figure 1c. In the Horn of Africa, the above-ground biomass can be less than 20% of the 15 year mean ( $AI_{AGB} < -80\%$ ) while for Australia wet case the anomaly is positive and in some area it exceeds the 15-years mean by 80%.

Another indicator of these extreme events is the NEE anomaly time series percentiles. For the two considered regions (Horn of Africa and central Australia), the 15-years mean NEE shows an overall respiration regime. Figure 3 shows the NEE anomaly time series with regard to the 15-years mean and its 10-90 and 30-70 percentiles. In the Horn of Africa (Figure 3 left) this anomaly is well above the 90<sup>th</sup> percentile of the whole 15-years which indicates an increase in the respiration regime obtained for the 15-years mean, this is also consistent with the LAI negative anomaly shown in Figure 1c. For the central Australia wet case (Figure 3 right), the anomaly is much smaller than the 10<sup>th</sup> percentile of the 15-years which corresponds to a decrease in the observed 15-years mean respiration regime and to the LAI positive anomaly (Figure 1c).

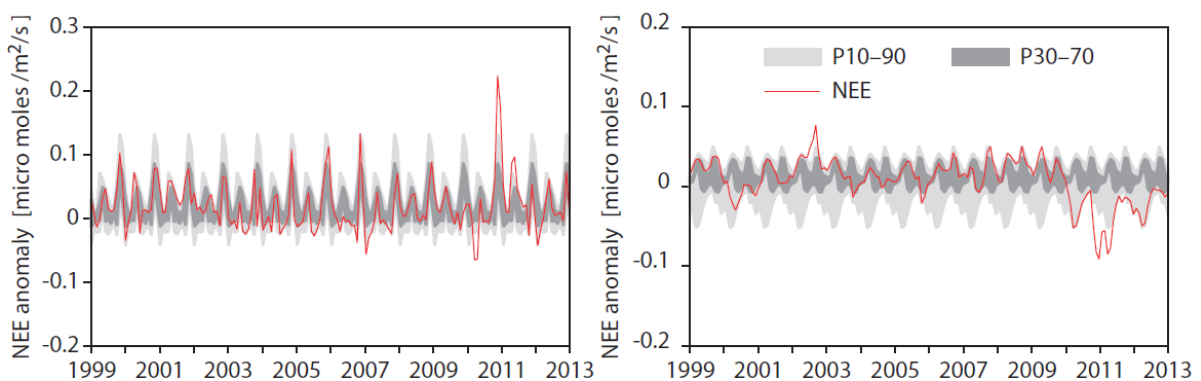


**Figure 3: Time series of the Net Ecosystem Exchange anomaly [ $\mu\text{mol m}^{-2} \text{s}^{-1}$ ] for the Horn of Africa (left), and for central Australia (right). Anomalies are shown as differences of absolute flux between simulation using climatological LAI and albedo and simulation using global LDAS.**

### 2.3.2. Comparison with WOFOST products

WOFOST is a crop growth model that allows estimating quantitatively yields, developed by the Department of Theoretical Production Ecology (Wageningen Agricultural University, The Netherlands) and the Center for Agrobiological Research and Soil Fertility (Wageningen, The Netherlands). This model is implemented currently within the MARS Crop Growth Monitoring System (CGMS), allowing the estimation of biophysical variables related with crop yields such as potential biomass production, crop development stage, etc...

WOFOST raw simulations were provided by JRC. They are done at soil unit level and multiple times for each of the soil types within a soil polygon. The WOFOST data were compared with the above-ground biomass outputs of CTESSEL when using climatological LAI (CTESSEL\_CLM) and when assimilating the NRT LAI through the Global LDAS system. Results were compared in term of absolute values and anomaly values with regard to 1999-2013 mean. Overall, compared to the WOFOST outputs, the LDAS is able to better capture the inter-annual variability than when using climatological LAI in CTESSEL (Figure 4 and Figure 5). The correlation with WOFOST outputs increases from 0.47 for CTESSEL\_CLM to 0.54 for LDAS. However, in term of absolute values, the above-ground biomass does not always match the WOFOST products as can be seen in the upper panels of Figure 4 and Figure 5. This could be related to several reasons among which the possible miss-match between the global vegetation map used in CTESSEL and the actual in-situ vegetation. In addition, although used as a benchmark, the WOFOST products are also model outputs which could also be contaminated with errors. This emphasizes the need for in-situ agricultural observations without missing the representativity issues that would arise when comparing point observations with global scale products.



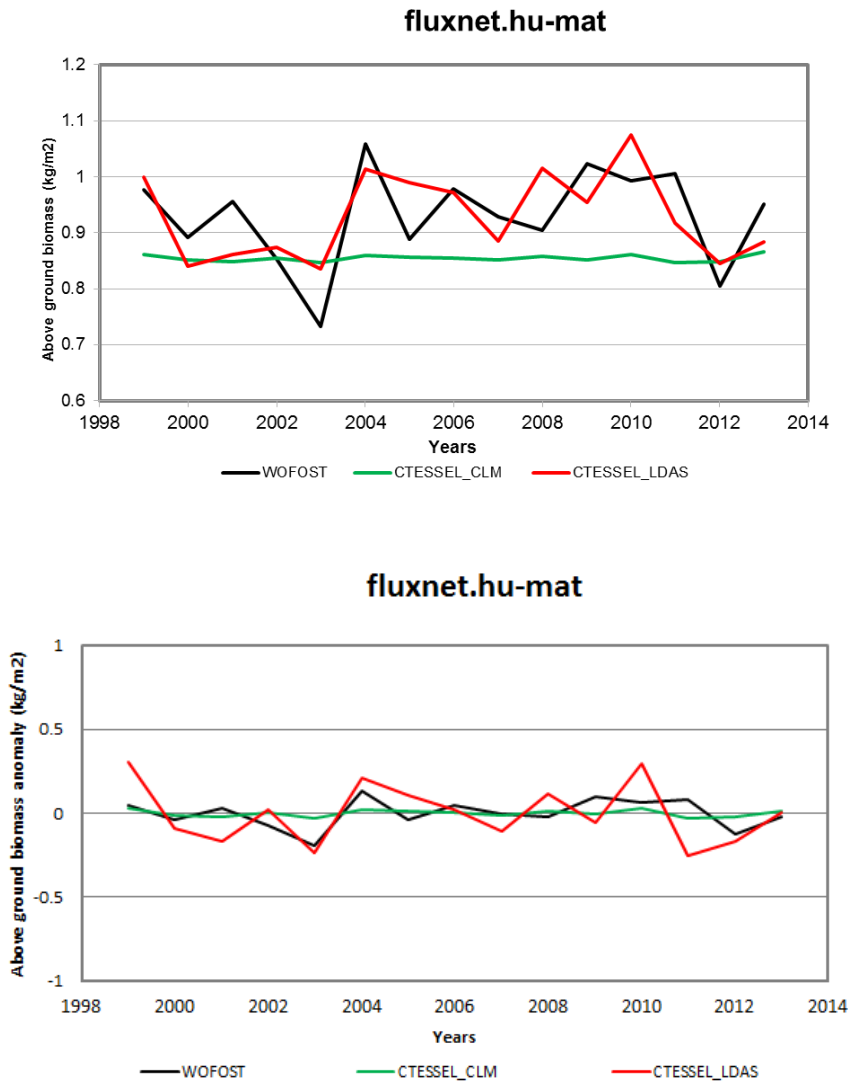


Figure 4: Comparison between WOFOST (black), CTESSEL with climatological LAI and albedo (green) and global LDAS (red) for the above-ground biomass (upper panel) and its anomaly with regard to the 1999-2013 mean (lower panel) at a FLUXNET Hungarian site.

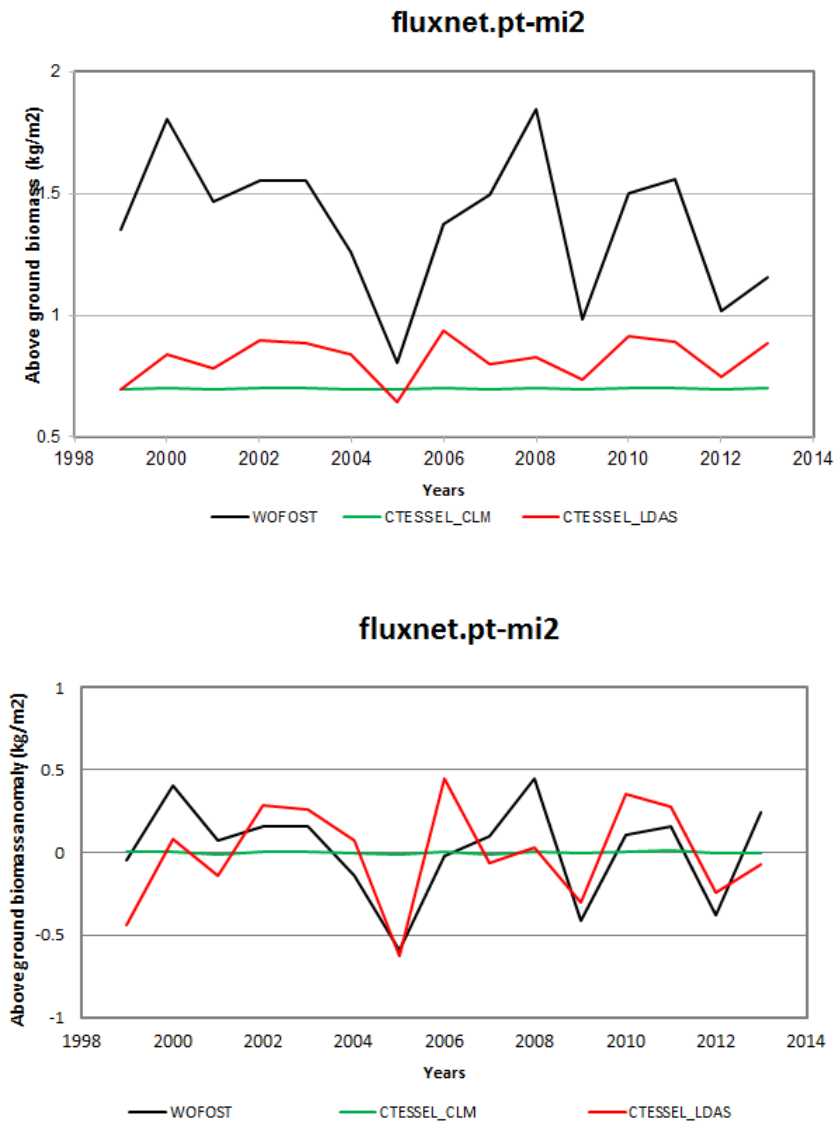


Figure 5: Same as Figure 4 for a FLUXNET Portuguese site.

## 2.4. ENERGY AND WATER

In order to assess the added value of the near real time LAI and albedo assimilation, the Global LDAS outputs were also evaluated against CTESSEL outputs, which are based on LAI and albedo climatology. A first assessment focus on the impact during extreme events such as the November 2010 Horn of Africa drought and Australia wet spell, then a second

assessment is performed based on comparison with in-situ FLUXNET observations. A third assessment is performed by comparing soil moisture outputs with the International soil moisture Network (ISMN) observations (Boussetta et al. 2015).

### 2.4.1. Energy and carbon Fluxes

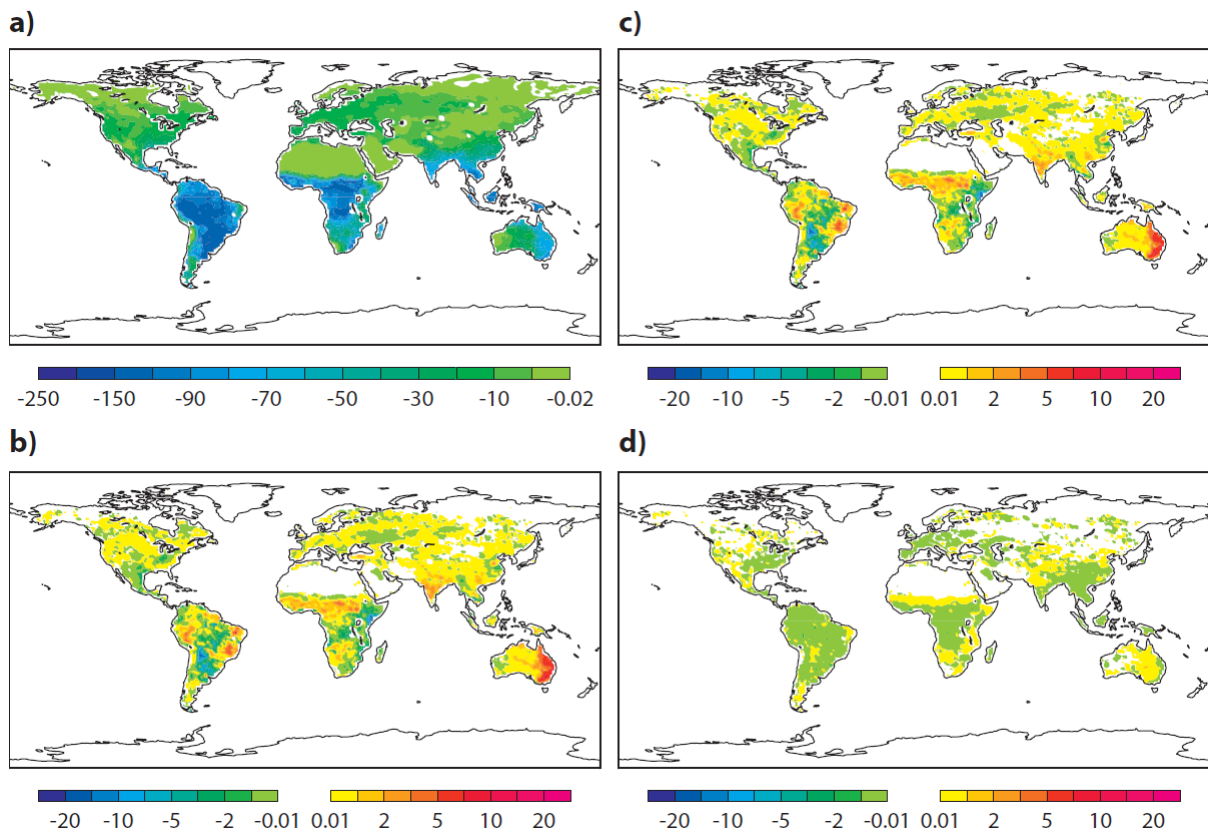


**Figure 6: Latent Heat flux [W m<sup>-2</sup>] for November 2010, a) using climatological LAI and albedo (SCLIM). Anomalies are shown as differences of absolute fluxes with respect to SCLIM for simulations using b) LAI and albedo NRT assimilation (SNRT), c) LAI NRT assimilation and albedo climatology (SLAINRT) and d) albedo NRT assimilation and LAI climatology (SLABNRT).**

Similar to the aboveground biomass (Figure 2) and the CO<sub>2</sub> flux (Figure 3), the energy fluxes were also affected by the LAI and albedo anomaly detected in November 2010 (Figure 1c). As a consequence to the observed decrease of LAI over the Horn of Africa, a decrease in the Latent heat flux (Figure 6b, c) and an increase in the sensible heat flux (Figure 7b, c) were obtained by the LDAS for both SLAINRT and SNRT configurations. The experiment using only the albedo NRT assimilation (SALBNRT) shows a minor decrease in both latent and sensible heat fluxes related to a mild increase of the surface albedo (Figure 1c) which induces a decrease in the net surface radiation.

albedo is due to the brightening of the surface caused by the drought condition. However, when combined, the NRT LAI and albedo (SNRT), the resultant anomaly signal of both latent (Figure 6b) and sensible heat fluxes (Figure 7b) is mainly driven by the LAI anomaly.

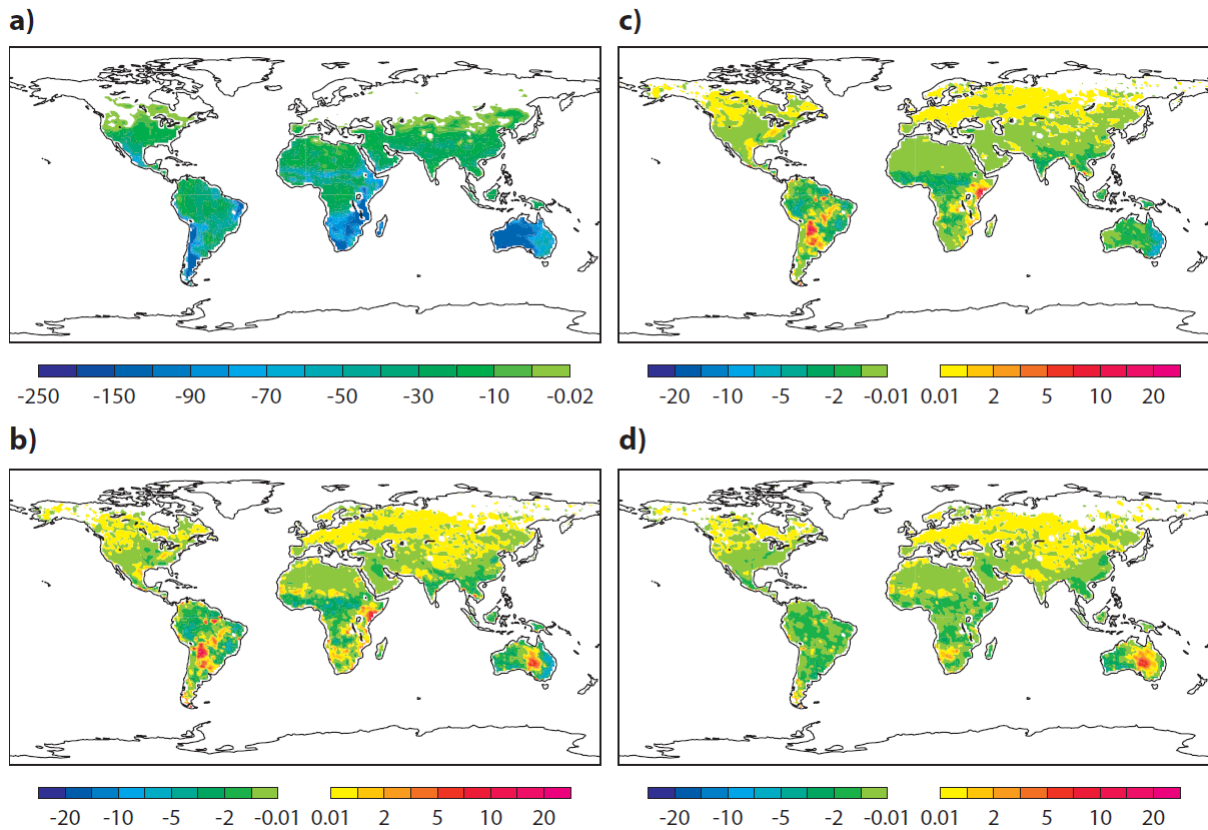


**Figure 7: Similar to Figure 6 for the Sensible Heat flux [ $W m^{-2}$ ].**

In the case of the wet anomaly over Australia, an opposite behavior is observed. The LAI positive anomaly in both SNRT and SLAINRT configurations resulted in an increase of the latent heat flux and a decrease of the sensible heat flux, especially over the densely vegetated area in the eastern region. In the central Australia region, which is less vegetated, the wet condition led to a decrease of the surface albedo resulting in an increase of the sensible heat flux (SALBNRT and SNRT). This effect was more important than the decrease caused by the LAI anomaly (SLAINRT) due to the small vegetation cover in this region as depicted in Figure 7.

Table 1 shows the benchmarking metrics of the LDAS outputs and CTESSEL simulations based on climatological fields against FLUXNET observations averaged over 52 sites for 2003 (Baldocchi et al. 2001 and Baldocchi, 2008). In this case, the observation sites were

mainly located in Europe and North America. Slightly better agreement with in-situ surface energy and CO<sub>2</sub> fluxes is obtained when LDAS is used, although the magnitude of the improvement is quite small and in some cases may not be within the significance range. For the energy fluxes, the use of the LDAS reduces the latent heat fluxes bias for 69% of the sites used in this comparison. In the case of the sensible heat fluxes, assimilating LAI NRT and albedo NRT reduces the bias for 67% of the sites while when using LAI NRT and albedo climatology the bias is reduced for 75% of the sites. The different simulation results have an equal average correlation over the 52 sites (0.85 for the latent heat flux, 0.74 for the sensible heat flux and 0.82 for the CO<sub>2</sub> flux). However, in terms of the number of sites with improved metrics, the correlation of the gross primary production increased for 57% of the sites when assimilating NRT LAI and albedo and for 63% of the sites when NRT LAI and albedo climatology are used.

**Table 1: Flux evaluation averaged against 52 FLUXNET sites for 2003: metrics based on 10-day averaged simulated fluxes. The Confidence Interval (CI) of RMSE is based on the Chi-squared distribution and the 95% CI of the mean correlation is based on the Fisher Z**

Flux	CTESSEL			LDAS-CTESSEL		
	RMSE	Bias	Corr.	RMSE	Bias	Corr.
<b>Latent Heat [W/m<sup>2</sup>]</b>	20.9 (±0.7)	10.40	0.85 (±0.01)	20.6 (±0.7)	9.60	0.85 (±0.01)
<b>N sites better than CTESSEL</b>	-	-	-	34	36	27
<b>Sensible Heat [W/m<sup>2</sup>]</b>	20.3 (±0.7)	-1.64	0.74 (±0.02)	20.4 (±0.7)	-1.77	0.74 (±0.02)
<b>N sites better than CTESSEL</b>	-	-	-	26	39	28
<b>Gross Primary Prod. [μmole/m<sup>2</sup>/s]</b>	2.06 (±0.07)	0.80	0.81 (±0.01)	2.12 (±0.07)	0.88	0.82 (±0.01)
<b>N sites better than CTESSEL</b>	-	-	-	25	18	33

## 2.4.2. Soil moisture

For the soil moisture benchmarking (Table 2), the signal of the improvement owing to the assimilation of NRT LAI and albedo is quite small although more than 50% of the modelled sites experienced a minor improvement in their correlation with the observed soil moisture. This signal is equally valid for the surface, which is evaluated against 523 sites of the ISMN and for the root-zone for which the evaluation is only performed on 58 sites of the USCRN network (Bell et al., 2013) given the availability of observations.

In addition, it is important to note that the metrics shown for the flux and soil moisture comparisons represent an average for all the sites considered for a full year. Therefore, the impact of any inter-annual variability or anomaly signal that NRT data may hold in some sites will be diluted with sites having a climatological year behavior. However, at the regional and global scales, an indirect assessment would be feasible by meteorologically evaluating the impact of assimilating LAI and albedo NRT on near-surface temperature and humidity forecasts.

**Table 2: Averaged metrics for surface and root-zone soil moisture benchmarking against the ISMN sites for 2010 based on daily soil moisture values. The confidence Interval (CI) of RMSE is based on the Chi-squared distribution and the 95% CI of the mean correlation is based on the Fisher Z.**

Soil moisture/Exp	CTESSEL			LDAS-CTESSEL		
	RMSE	Bias	Corr.	RMSE	Bias	Corr.
<b>Surface ( 523 sites)</b>	0.138 (±0.0004)	-0.108	0.688 (±0.002)	0.137 (±0.0004)	-0.107	0.690 (±0.002)
<b>N sites better than CTESSEL</b>	-	-	-	297	293	307
<b>Root zone (58 sites)</b>	0.114 (±0.001)	-0.064	0.698 (±0.007)	0.113 (±0.001)	-0.062	0.700 (±0.007)
<b>N sites better than CTESSEL</b>	-	-	-	33	34	32

## 2.5. FORECAST IMPACT OF GLOBAL LAND PRODUCTS

To evaluate the impact of the assimilation of NRT LAI and albedo on the surface–atmosphere interaction, a series of 3-days forecasts initialised every day from 1<sup>st</sup> January 2010 00UTC to 31<sup>st</sup> December 2010 00UTC was performed using the different LAI and albedo products. The ECMWF IFS was used for these forecasts simulations. Given the different time scales between land surface processes and atmosphere, and to avoid spin-up problems related to slow surface processes, the surface initial conditions of each forecast experiments are obtained from the corresponding surface offline simulations. The focus is on short-range forecasts, which have the advantage that the synoptic situation is in the predictable range. Still, changes in albedo and LAI would have an impact on near-surface atmosphere through radiative forcing and sensible and latent heat flux. Screen-level

temperature and moisture can be verified using the analysis, which draws closely to the surface synoptic observations. The model is run with 137 vertical levels at ~40 km horizontal resolution. The assessment of the impact of LDAS is done for the screen-level temperature and relative humidity through two metrics named hereafter sensitivity and impact:

$$sensitivity(T) = T_{exp} - T_{ctl} \quad (1)$$

$$impact(T) = |T_{exp} - T_{an}| - |T_{ctl} - T_{an}| \quad (2)$$

Where subscripts *ctl* refers to climatological LAI/albedo based forecast, *exp* refers to LDAS's LAI/albedo based forecast and "*an*" refer to the operational analysis. The equivalent quantities are computed for relative humidity. Therefore a positive (negative) sensitivity would mean an increase (decrease) of temperature/relative humidity at the 2-m level due to assimilation of the NRT data. A positive (negative) value of the impact means an increase (reduction) of the 2-m temperature/relative humidity error in comparison to the operational analysis due to the use of the LDAS.

Figure 8 shows the results of the forecast experiment using the assimilated LAI NRT (FLAINRT) for the global land for the 36-hours forecast (valid at 12 UTC) in comparison to the control run FCLIM where LAI climatology is used for November 2010. The use of LDAS LAI results in a neutral to positive impact for the global 2-m temperature (Figure 8c). In this case, the bias reduction corresponds to a temperature change that reaches 2 K caused by the LAI anomaly, with a warming over the Horn of Africa co-located with the LAI reduction and a cooling co-located with the LAI positive anomaly over eastern Australia (Figure 8a). The African tropics also experiences a cooling partially related to a positive LAI anomaly which contributes in reducing the temperature bias in comparison with the operational analysis. However, a similar cooling over the Indian peninsula results in a mild bias increase of 0.2 K. The relative humidity results show similar patterns. The regions, which have a temperature increase, display a drying in the relative humidity, while the regions that have a cooling show a moistening in the relative humidity (Figure 8b). As for the temperature results, the changes in the relative humidity, which are co-located with the LAI anomaly, correspond in general to a bias reduction in comparison with the operational analysis relative humidity (Figure 8d).



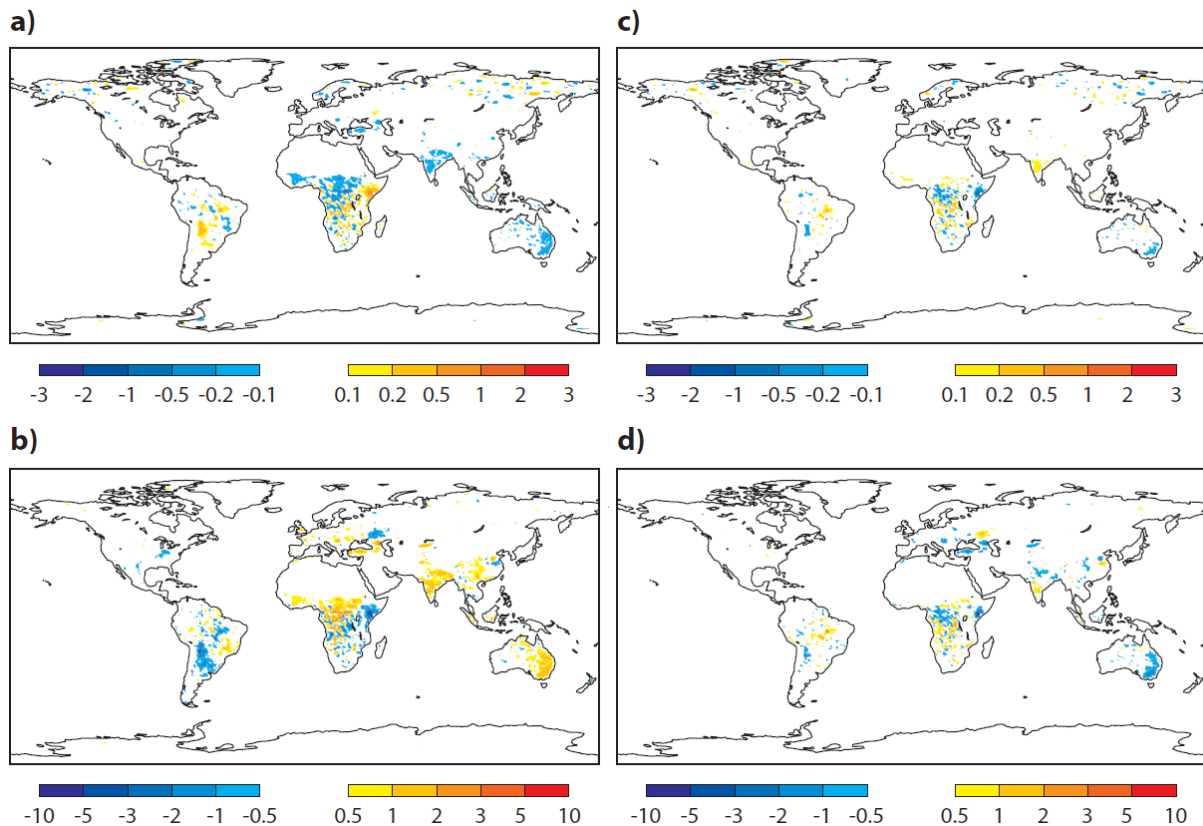


**Figure 8: Scores of forecast experiment using LDAS LAI (FLAINRT) against experiment using LAI climatology (FCLIM) for November 2010: a) 2-m temperature sensitivity [K], b) 2-m relative humidity sensitivity [%], c) 2-m temperature impact, and d) 2-m relative humidity impact. (A positive/negative value of the impact means an increase/reduction of the 2-m temperature/relative humidity error in comparison to the operational analysis).**

In the case of the FNRT forecast experiment where both assimilated LAI and albedo NRT are used, the results are quite similar to the FLAINRT experiment where only LAI inter-annual variability is represented while albedo is climatology (Figure 9). The only noticeable difference can be seen over central and eastern Australia where the negative albedo anomaly occurs; in this case, the cooling/moistening (Figure 8a/b) caused by the LAI positive anomaly is reduced and even reversed compared to FLAINRT (Figure 9a/b). This can be explained by the darkening of the surface albedo (Figure 1c), which causes an increase of the absorbed surface radiation and consequently an increase in the sensible heat flux as depicted in the offline experiment (Figure 7). The positive impact related to this sensitivity is in general preserved (Figure 9c,d) except in central Australia where the warming/drying mildly increases the temperature/relative humidity bias compared to the operational analysis.



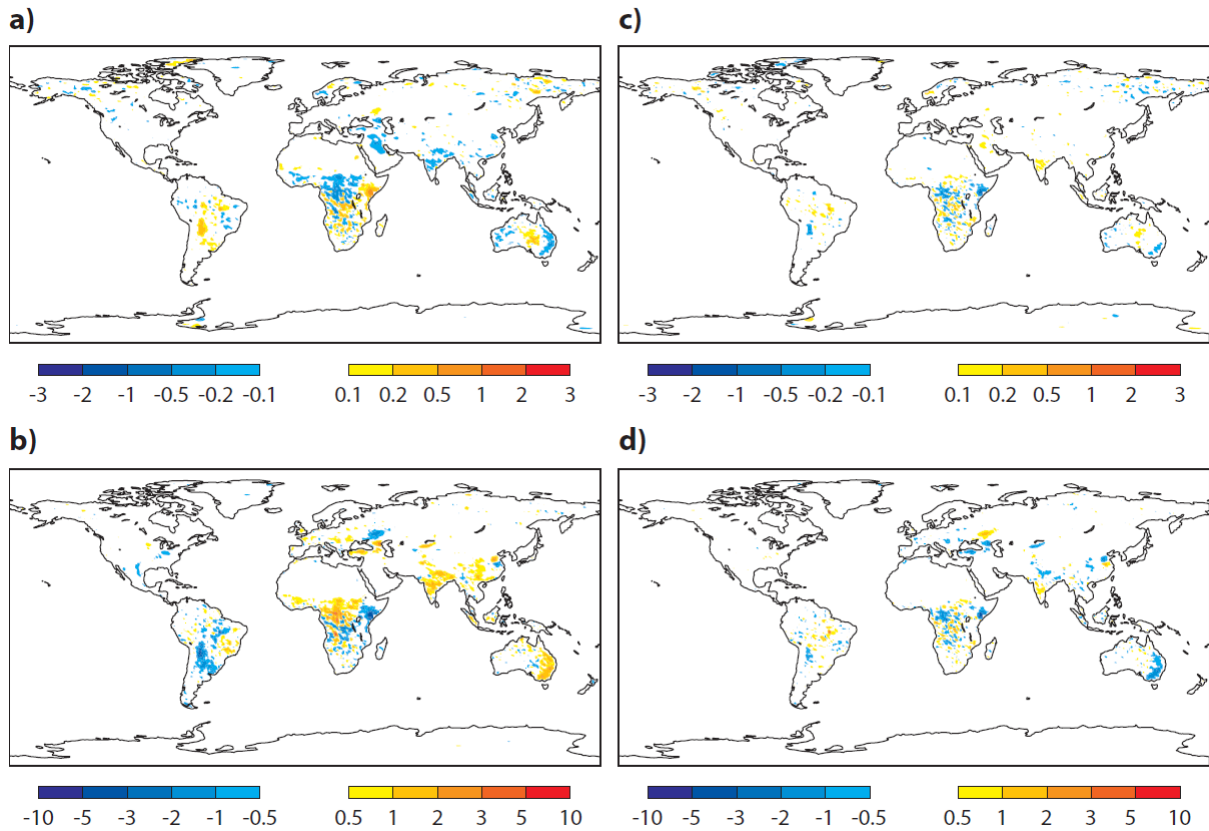


**Figure 9: Scores of forecast experiment using LDAS LAI and albedo (FNRT) against experiment using climatology (FCLIM) for November 2010: a) 2-m temperature sensitivity [K], b) 2-m relative humidity sensitivity [%], c) 2-m temperature impact, and d) 2-m relative humidity impact. (A positive (negative) value of the impact means an increase (reduction) of the 2-m temperature/relative humidity error in comparison to the operational analysis).**

### 3. CONCLUSIONS AND PERSPECTIVES

The ECMWF global land surface modeling and assimilation system is used as a platform to ingest the Earth Observations products produced within the Copernicus Global Land Services. The motivations are given by the need to improve the Earth System simulations and given the important role of LAI and albedo in the radiative forcing and the surface energy, water and carbon budgets, it is expected that, compared to the climatological fields, the assimilation of NRT LAI and albedo would have an impact on surface carbon and energy fluxes and subsequently affect the prediction of the near-surface atmosphere as well as above-ground biomass.

In the framework of IMAGINES, it was shown that the assimilation system is able to correct deficiencies in the satellite observation products, especially in high latitudes and snow covered areas as well as in the cloud-contaminated areas. The final products have smoother spatial and temporal evolution, which make them more appropriate for environmental and numerical weather prediction.

The LDAS showed an added value in detecting/monitoring extreme drought and wet events and improves the correlation between the above-ground biomass and the WOFOST products.

The LDAS runs show that extreme NRT LAI anomalies have a strong impact on the surface energy and CO<sub>2</sub> fluxes, larger than the albedo anomalies, which have a smaller range. In addition, an evaluation against in-situ observations showed that a neutral to slightly better fit with in-situ surface soil moisture (from ISMN) and surface energy and CO<sub>2</sub> fluxes (from FLUXNET) can be obtained when assimilating NRT products although the average signal can be weakened from non-anomalous areas/sites. The offline surface runs and forecasts experiments confirm the benefit coming from a more realistic treatment of vegetation by the use of NRT LAI and albedo through the LDAS system. Using the LDAS, anomalous years could be detected and surface fluxes were directly affected by their inter-annual variability. The forecast simulation confirmed this positive impact on the near-surface weather parameters and its potential to account for NRT issues such as a rapid change in the LAI due to fast growth or harvest as well as inter-annual variability due to an extreme drought or an extensive snow season that may inhibit growth.

Substantial research and operational consolidation of the processing chains are necessary to establish a continuous operational uptake of the NRT Copernicus Global Land products and Horizon 2020 framework program together with the Copernicus services will support further integrations within ECMWF forecast systems.

## 4. REFERENCES

Baldocchi, D., et al., (2001). FLUXNET: A new tool to study the temporal and spatial variability of ecosystem-scale carbon dioxide, water vapor, and energy flux densities. *Bull. Am. Meteorol. Soc.*, 82, 2415-2434, doi:10.1175/1520-0477.

Baldocchi D., (2008). Breathing of the terrestrial biosphere: lessons learned from a global network of carbon dioxide flux measurement systems. *Aust. J. Bot.*, 56, 1–26.

Balsamo, G., Viterbo, P., Beljaars, A., van den Hurk, B., Hirschi, M., Betts, A. K., & Scipal, K. (2009). A Revised Hydrology for the ECMWF Model: Verification from Field Site to Terrestrial Water Storage and Impact in the Integrated Forecast System. *J. Hydrometeorol.*, 10, 623-643.

Balsamo, G., Boussetta, S., Dutra, E., Beljaars, A., Viterbo, P. & Van den Hurk, B. (2011). Evolution of land surface processes in the IFS, *ECMWF Newsletter*, 127, 17-22.

Barbu, A. L., Calvet, J.-C., Mahfouf, J.-F., and Lafont, S. (2014): Integrating ASCAT surface soil moisture and GEOV1 leaf area index into the SURFEX modelling platform: a land data assimilation application over France, *Hydrol. Earth Syst. Sci.*, 18, 173-192, doi:10.5194/hess-18-173-2014.

Bell, J. E., Palecki, M. A., Baker, C. B., Collins, W. G., Lawrimore, J. H., Leeper, R. D., Hall, M. E., Kochendorfer, J., Meyers, T. P., Wilson, T. & Diamond, H. J. (2013). U.S. Climate Reference Network soil moisture and temperature observations. *J. Hydrometeorol.*, 14, 977-988. doi: 10.1175/JHM-D-12-0146.1.

Bolten, J. D. and Crow, W. T. (2012): Improved prediction of quasi-global vegetation conditions using remotely-sensed surface soil moisture, *Geophys. Res. Lett.*, 39, L19406, doi:10.1029/2012GL053470.

Boussetta, S., Balsamo, G., Beljaars, A., Kral, T. & Jarlan, L. (2013). Impact of a satellite-derived Leaf Area Index monthly climatology in a global Numerical Weather Prediction model, *Int. J. Rem. Sens.*, 34 (9-10), 3520-3542.

Boussetta, S., Balsamo, G., Dutra, E., Beljaars, A., Albergel, C., (2015). Assimilation of surface albedo and vegetation states from satellite observations and their impact on numerical weather prediction, *Remote Sensing of Environment*, Volume 163, 15 June 2015, Pages 111-126, ISSN 0034-4257, <http://dx.doi.org/10.1016/j.rse.2015.03.009>.

Calvet, J.-C., Lafont, S., Cloppet, E., Souverain, F., Badeau, V., and Le Bas, C. (2012): Use of agricultural statistics to verify the interannual variability in land surface models: a case study over France with ISBA-A-gs, *Geosci. Model Dev.*, 5, 37–54, doi:10.5194/gmd-5-37-2012.

De Rosnay, P., Drusch, M., Vasiljevic D., Balsamo, G., Albergel, C., Isaksen, L. (2013): A simplified extended Kalman filter for the global operational soil moisture analysis at ECMWF. *Q J R Meteorol Soc.* Doi : 10.1002/qj.2023.

Deardorff, J.W., (1978). Efficient prediction of ground surface temperature and moisture, with inclusion of a layer of vegetation. *J. Geophys. Res.*, 83, 1889-1903.

Draper, C., Mahfouf, J.-F., Calvet, J.-C., Martin, E., and Wagner, W. (2011): Assimilation of ASCAT near-surface soil moisture into the SIM hydrological model over France, *Hydrol. Earth Syst. Sci.*, 15, 3829–3841, doi:10.5194/hess-15-3829-2011.

Pielke, R.A., and R. Avissar, 1990: Influence of landscape structure on local and regional climate. *Landscape Ecology*, 4, 133-155.

Sawada Y, T Koike, PA Jaranilla-Sanchez (2014): Modeling hydrologic and ecologic responses using a new eco-hydrological model for identification of droughts. *Water Resources Research*.

## ACKNOWLEDGEMENT

The authors thank Bettina Baruth, from JRC, for having provided the WOFOST simulations. The ImagineS coordinator, Dr. Roselyne Lacaze, and the data-handling specialists at VITO, Bruno Smets and colleagues, are acknowledged for their seamless support throughout this project. We thank our LDAS colleagues, Dr. Jean-Christophe Calvet, Dr. Alina Barbu, Dr. Helga Toth, for fruitful discussions of the scientific advances within ImagineS project.

This work used eddy covariance data acquired by the FLUXNET community and in particular by the following networks: AmeriFlux (U.S. Department of Energy), Biological and Environmental Research, Terrestrial Carbon Program (DE-FG02-04ER63917 and DE-FG02-04ER63911), CarboItaly, CarboMont, Fluxnet-Canada (supported by The Canadian Foundation for Climate and Atmospheric Sciences (CFCAS), The Natural Sciences and Engineering Research Council of Canada (NSERC), BIOCAP Foundation, Environment Canada, and Natural Resources Canada (NRCan)), the Sources and Sinks of Greenhouse Gases from managed European Grasslands and Mitigation Strategies (GreenGrass) project, the Large-scale Biosphere-Atmosphere Experiment in Amazonia (LBA), the Nordic Centre for Studies of Ecosystem carbon exchange and its Interaction with the Climate system (NECC), the Terrestrial Carbon Observation System Siberia (TCOS-Siberia). We thank in particular the PIs that decided to share their data freely within the scientific community. We acknowledge the support to the eddy covariance data harmonization provided by the Integrated Project Assessment of the European Terrestrial Carbon Balance (CarboEuropeIP), The Food and Agriculture Organization-The Global Terrestrial Observing System-The Terrestrial Carbon Observations project (FAO-GTOS-TCO), the Integrated Land Ecosystem-Atmosphere Processes Study (iLEAPS), Max Planck Institute for Biogeochemistry, National Science Foundation, University of Tuscia, Université Laval and Environment Canada and US Department of Energy and the database development and technical support from Berkeley Water Center, Lawrence Berkeley National Laboratory, Microsoft Research eScience, Oak Ridge National Laboratory, University of California - Berkeley, University of Virginia. We also thank The Fluxnet-Canada Research Network for making available the BERMS data ( <http://berms.ccrp.ec.gc.ca/Overview/e-overview-about.htm> ), the PIs and researchers involved in the Coordinated Enhanced Observing Period (CEOP) project for provision and archiving of the data used in this study ( <http://www.ceop.net/> ), and the CARBOSCOPE project contributors for making their data freely available through the project website ( <http://www.carboscope.eu/?q=home> ). We thank also all the PIs of the International Soil Moisture Network (ISMN) that decided to share their data freely within the scientific community (<https://ismn.geo.tuwien.ac.at/ismn/>).